6

Ultra-Wideband Automotive Radar

Akihiro Kajiwara
The University of Kitakyushu
Japan

1. Introduction

A lot of progress has been made for automotive radar during the last years. There are two types of automotive radar; "long-range radar at 77GHz with a range capability up to 200m" for automatic cruise control (ACC) and "short-range radar at 24/26 and 79GHz up to 30m" for anti-collision. Long radar with narrow radiation beam enables a automobile to maintain a cruising distance, while short-range radar has recently attracted attention because of many applications such as pre-crush warning, stop-and-go operation and lane change assist. The short-range radar with a very broad lateral coverage has a few significant problems to be overcome such as target detection and clutter suppression. This is because the widely radiated radar echo contains not only automobile echo, but also unwanted echoes called clutter. It is actually not easy to detect a target echo in increased clutter. Ultra-wideband impulse-radio (UWB-IR) radar with high range-resolution has recently attracted much attention for automotive use, because it offers many applications such as pre-crush warning and lane change assist.

The followings provide an overview of this chapter;

1. Section 2 introduces various radar systems for automotive use. It begins with a discussion of radar technologies such as Pulse Doppler, FM-CW and UWB-IR.
2. UWB-IR radar requires high speed A/D devices which can directly process the received nanosecond pulse. For example, A/D devices of several GS/s or more should be required for the UWB-IR radar with a bandwidth of 1GHz, which have not been available yet. The use of wideband may also cause unacceptable interference on existing narrowband systems. Therefore, some interference mitigation scheme may be required for the radar emission in the future. To solve these problems, a stepped-FM radar scheme is introduced in Section 3, which does not require high speed A/D device and provides the co-existence with exisiting narrowband systems.
3. Short range radar is expected to provide a ***wide*** coverage in azimuth ***angle.*** Therefore, increased clutter makes it difficult to detect automobile target accurately. The clutter can be classified from automobile by the Doppler, but it will not be applicable to the UWB-IR. In Section 4, a scheme is introduced which estimates the Doppler by using the time-trajectory of radar echo and the measurement results are presented.
4. Automotive radar is required to detect automobile accurately, but not to detect clutters falsely, even in complicated traffic conditions. In order to satisfy the requirement, a target discrimination scheme with range profile matching is introduced in Section 5 and the measurement results are presented. The results show that the automobile type can be discriminated.

2. Fundamentals of radar technologies

2.1 Radar detection

The basic principle of UWB-IR automotive radar detection is illustrated in Fig.1 where the received signal includes many echoes scattered from desired and undesired objects (Skolnik, 2001) (Taylor, 1995). The one-dimensional signal, which is referred to as range profile, is generally presented by multiple impulses with gains $\{\beta_k\}$ and propagation delays $\{\tau_k\}$, where k is the impulse index. Suppose a nanosecond pulse of $s(t)$, the range profile, $y(\tau, t)$, is the time convolution of $s(t)$ and the impulse echo response $\Sigma\beta_k\delta(t-\tau_k)$ as follows;

$$y(\tau,t)=\sum_k \beta_k s(t-\tau_k) \tag{1}$$

Fig.1 (b) shows an example of received power range profile for a bandwidth of 1GHz (corresponding to 1 nanosecond pulse) on a roadway.
When a target echo exceeds a given threshold, it can be recognized. However if a clutter echo exceeds the threshold, it is mistaken as a target. This is called a missed detection. Consider the target detection in increased clutter as shown in Fig.1, it is not easy to recognize the automobile target since the echoes over a threshold can't be classified usually as target or clutter.

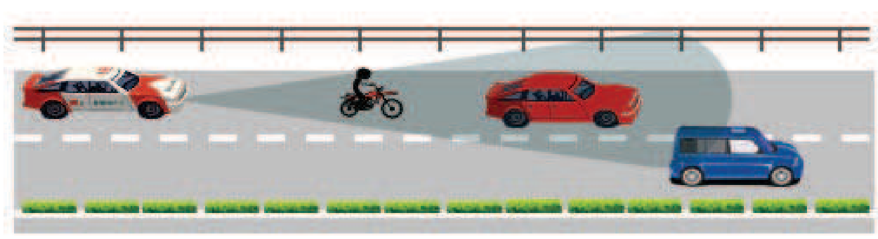

(a) Automobile radar image

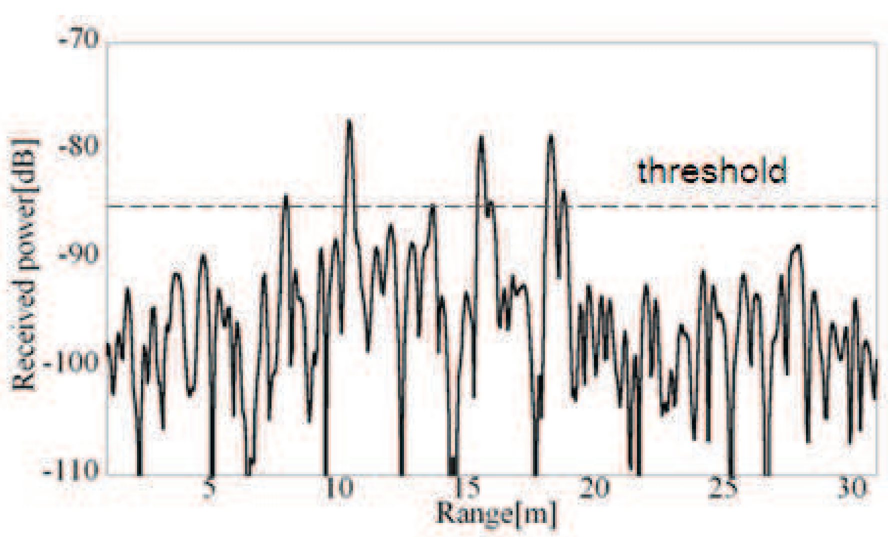

(b) Power range profile

Fig. 1. Principle of radar detection

The typical radar utilizes a pulse waveform. The transmitted pulse is intercepted by some objects and re-radiated in many directions. The re-radiation directed back towards the radar is collected by the directional antenna. The received signal is then processed to detect the presence of target on the threshold basis. The range to a target is estimated by measuring the travelling time from the transmitter to the receiver. The range is given by $d = c\tau / 2$ where τ is the time and c is the speed of light. The radar equation generally relates the detectable range. It is useful not only for determining the maximum range at which the radar can detect a target, but it can serve as a means for understanding the factors affecting radar performance. For the transmit power P_t in a particular direction, the maximum gain G of antenna and the received signal P_r at a range d is given by (Skolnik,2001)

$$P_r = \frac{P_t \cdot G^2 \cdot \sigma \cdot \lambda^2}{(4\pi)^3 d^4}, \tag{2}$$

where λ is the wavelength and σ denotes the reflectivity of the target which is also called radar cross section (RCS).

The RCS depends on the target shape, λ and radar bandwidth. An example of the measured RCS of a sedan type of automobile is shown in Fig.2, where we considered a CW of 25.5GHz and UWB of 22-29GHz (Matsunami et al., 2008). Change in the RCS of the CW is found to be significant to the azimuth angle, while the RCS forof the UWB is much less sensitive to the azimuth angle relative to the CW.

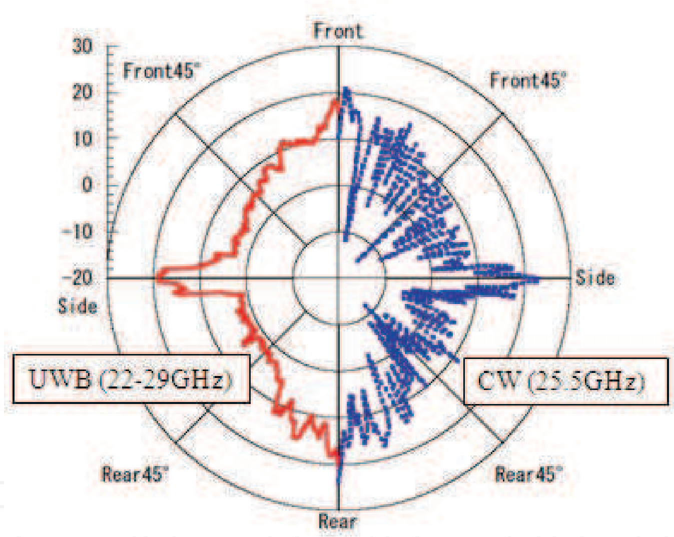

Fig. 2. Azimuth variation of the RCS of a sedan typed automobile

2.2 Automotive radar system

There are several types of radar systems and a large number of different applications. In this section, three types of radar system are discussed: Pulse Doppler, FM-CW and UWB-IR radar systems.

Pulse Doppler radar

Pulse Doppler radar sends out a pulse train. When the transmit pulse is long enough and the target’s Doppler is large enough, it may be possible to detect the Doppler shift on the basis of the frequency change within a single pulse. Fig.2-3 (b) shows that there is a recognizable Doppler shift in frequency domain. To detect the Doppler on the basis of a single pulse of width T_p generally requires that there be at least one cycle of the Doppler frequency f_d within the pulse. Also, the transmit frequency source must have very good phase stability and the system is required to be coherent. Fig. 3 illustrated the principle of Pulse Doppler where the pulse repetition period is T. For a moving target, the received echo experiences a Doppler f_d as shown in Fig.2-3. Therefore the Doppler can be estimated by processing the received echo in frequency domain.

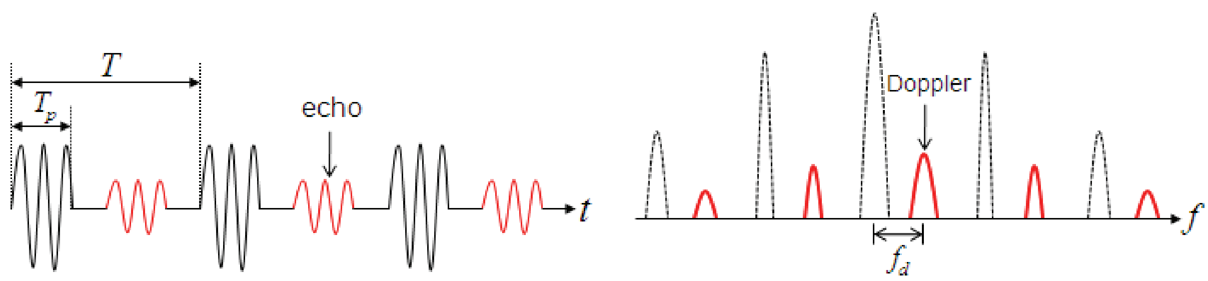

Fig. 3. Principle of Pulse Doppler radar

FM-CW radar

FM-CW (Frequency-modulated continuous-wave) radar system varies the frequency of the transmit signal and measures the range based on the frequency difference between the instantaneous transmit signal and received echo. The typical modulations includes triangular and saw-tooth. Current applications of FM-CW include high-resolution systems. Fig. 4 (a) shows the block diagram of a typical triangular FM-CW radar where the super-heterodyne-receiver is assumed. The frequency-analyzed beat signals for up-frequency and down-frequency are passed through an A/D device, and digital processing of FFT is then conducted. Please note that the beat signal exhibits a peak at which the intensity becomes large corresponding to the target. And the peak frequency corresponding to this peak carries information concerning the distance, and the peak frequency differs between the up portion and down portion of the triangular FM-CW wave due to the Doppler associated with the relative velocity of a target.

The up-beat α is given by the followings;

$$\alpha = f_1 - f_2 = \frac{\Delta f}{T_m} \cdot \frac{2d}{c} - f_d \tag{3}$$

$$f_1 = \frac{\Delta f}{T_m} t \tag{4}$$

$$f_2 = \frac{\Delta f}{T_m}\left(t - \frac{2d}{c}\right) + f_d, \tag{5}$$

where Δf is the frequency excursion.

The down-beat β is also given by

$$\beta = f_2 - f_1 = \frac{\Delta f}{T_m} \cdot \frac{2d}{c} + f_d \tag{6}$$

$$f_1 = -\frac{\Delta f}{T_m}(t - T_m) + \Delta f \tag{7}$$

$$f_2 = -\frac{\Delta f}{T_m}\left(t - T_m - \frac{2d}{c}\right) + \Delta f + f_d \tag{8}$$

From the above α and β, the Doppler f_d and the distance d to a target are derived as follows;

$$f_d = \frac{1}{2}(\beta - a)$$
$$d = \frac{cT_m}{4\Delta f}(\beta + a) \tag{9}$$

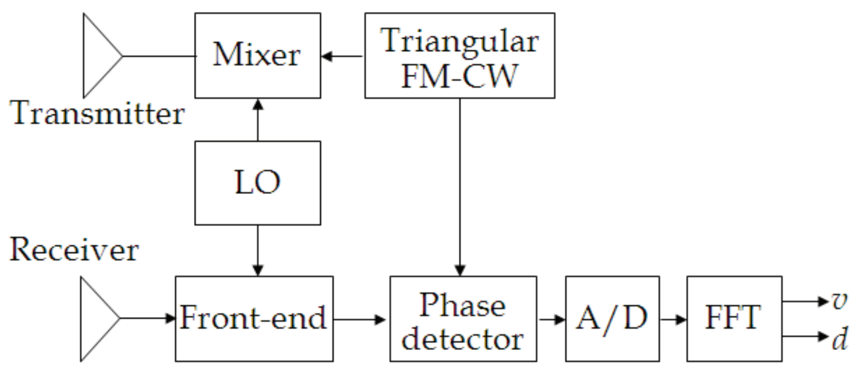

(a) Block diagram of triangular FM-CW radar

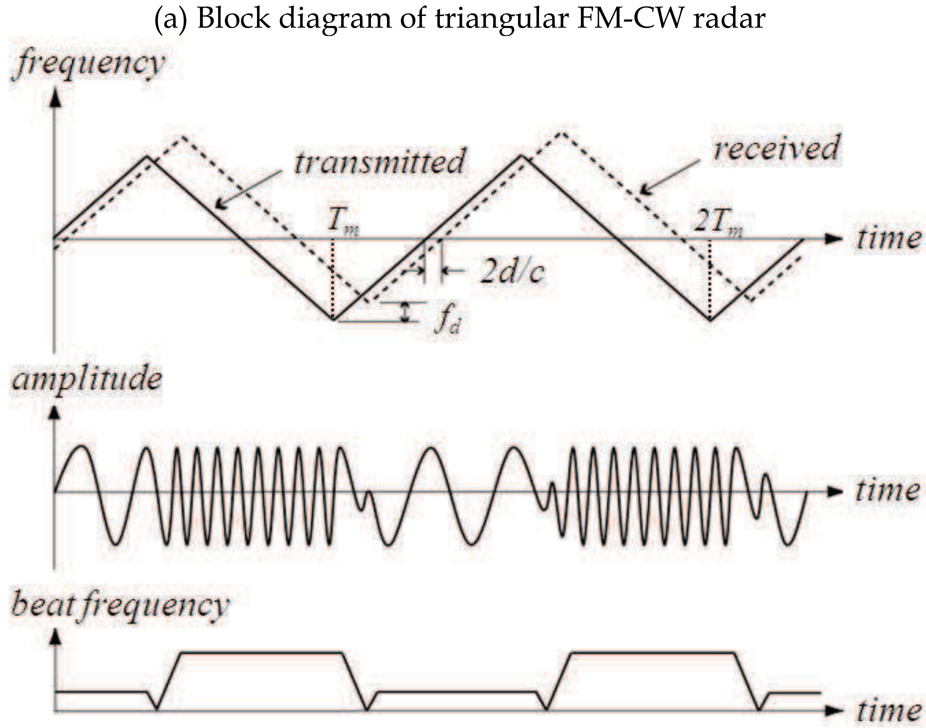

(b) Frequency-time relation for triangular FM-CW

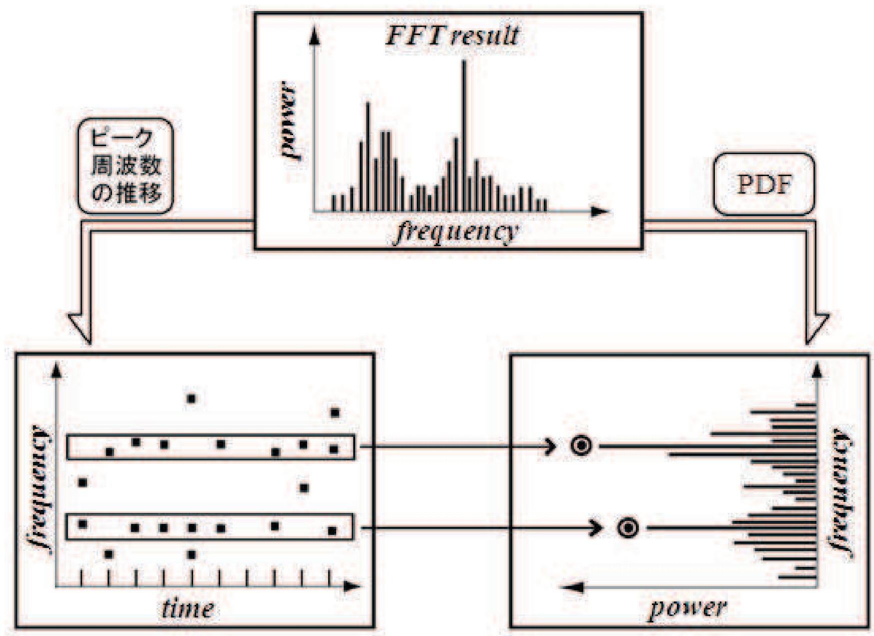

(c) Frequency-time relation

Fig. 4. FM-CW radar

If there is more than one autobile traveling in front, one pair of peak frequencies, one in the up portion and the other in the down portion, occurs for each automobile. The pairing of the peak frequencies between the up and down portions is done on an automobile-by-automobile basis. The pairing is performed based on the peak frequencies as shown in Fig. 4 (c), and the range and relative velocity of the corresponding automobile are determined. However the selection requires complicated processing.

UWB-IR radar

UWB-IR radar system transmits signals across a much wider frequency than conventional signals. The transmit signal is significant for its very light power spectrum which is typically lower than -41.3dBm. The most common technique for generating a UWB-IR signal is to

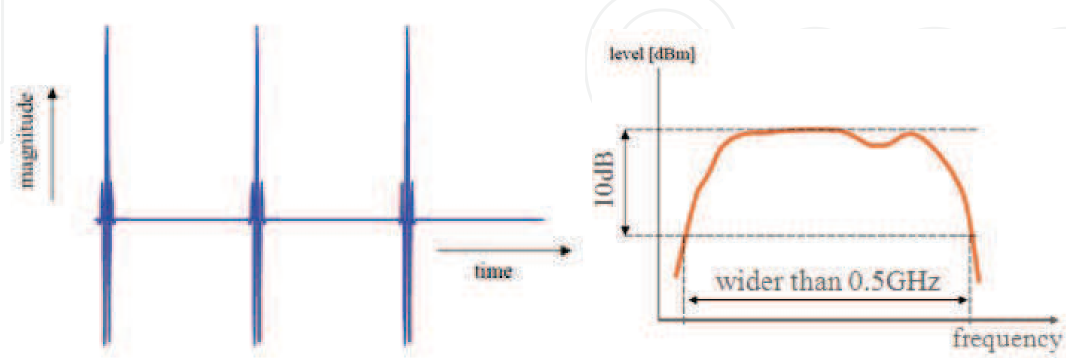

Ultra-short pulse (b) Power spectrum

Fig. 5. Train of ultra-short pulses and its spectrum

transmit a very short pulse train (less than 1nanosecond). The spectrum of a very narrow-width pulse has a very large frequency spectrum approaching that of white noise as the pulse becomes narrower and narrower. These very short pulses need a wide bandwidth as shown in Fig.5. The amount of spectrum is at least 25% of the center frequency. For the high range-resolution radar with wider than 1GHz, each scattered echo should be separated. Fig.6 shows the range profiles of a roadway where an automobile target was located at 10m. The measurement was conducted for various bandwidths of 100MHz to 5GHz (Matsunami et al., 2008). It is seen that the echoes for various objects can be separated using a shorter pulse.

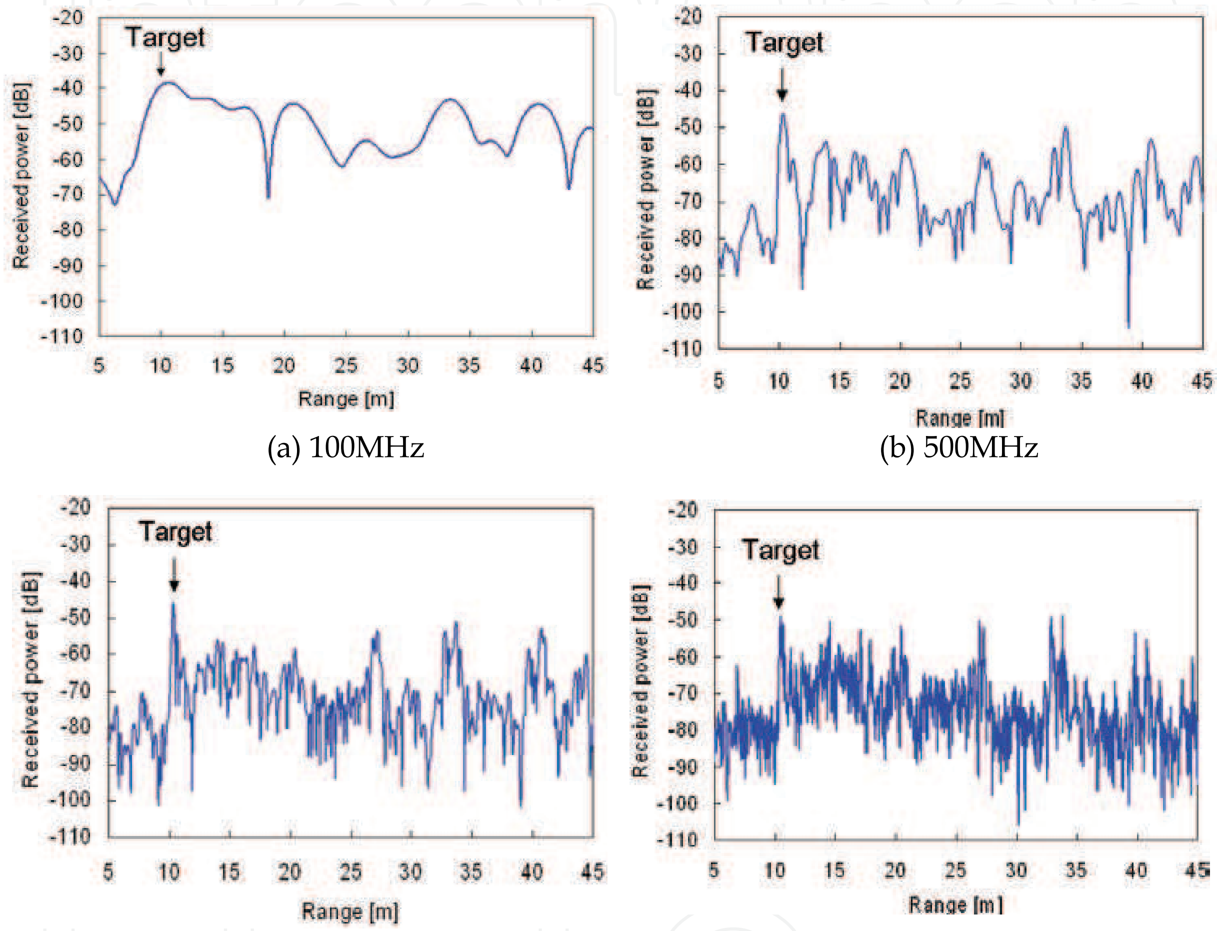

(a) 100MHz (b) 500MHz

(c) 1GHz (d) 5GHz

Fig. 6. Power delay profiles for automobile

3. Stepped-FM radar

UWB-IR radar provides multipath tolerability and high range-resolution, but it requires high speed A/D devices which can directly process the received nanosecond pulse. For example, A/D devices of several GS/s or more should be required for the UWB-IR radar with a bandwidth of 1GHz, which have not been available yet. Please note that it is difficult to realize analogue devices which can process such wideband pulse. The use of wideband would also cause unacceptable interference on existing narrowband systems. Therefore, some interference mitigation scheme may be required for the wideband radar emission in the future. To solve these problems, stepped-FM radar is introduced which does not require high speed A/D device and provides the co-existence with exisiting narrowband systems.

3.1 Stepped-FM scheme

The block diagram and each signal waveforms are shown in Fig.7. The stepped-FM radar transmits a series of bursts of narrowband pulses, where each burst is a sequence consisting of N pulses shifted in frequency from pulse to pulse with a fixed frequency step Δf . The received echo from a target is phase-detected into a train of narrowband base-band pulses and is then I-Q sampled by a relaxed speed of A/D. Each complex sample is applied to the inverse discrete Fourier transformation (IDFT) device in order to obtain an N-element synthetic range profile, which is called range spectrum, where the range resolution becomes approximately $1/N\Delta f$ (Nakamura et al., 2010) (Wehner, 1995). For example, suppose Δf =34.5MHz and N=30, the resolution is approximately 30 cm which is equivalent to a very short pulse with 1GHz. Therefore it does not require high speed A/D devices at the receiver.

The received stepped pulses are phase-detected and the resulting video pulses are then I/Q sampled. The n-th complex sample R_n is given by

$$R_n = A_n \exp(-j\phi_n) \tag{11}$$

$$\phi_n = 2\pi\left(f_c + (n-1)\Delta f\right)\cdot\frac{2d}{c}, \tag{12}$$

where A_n is amplitude of n-th pulse (For a stationary target, A_n should be approximated by A), f_c is fundamental frequency and c is velocity of light. Therefore received pulses (n = 1, 2,…,N) are denoted by $N\Delta f$ at frequency domain and the range-resolution ΔR is given by

$$\Delta R = \frac{c}{2N\Delta f} \tag{13}$$

Then, N complex sample is applied to the following IDFT device in order to obtain an N-element range spectrum.

$$\begin{aligned} R(\varphi) &= \left|\sum_{n=1}^{N} R_n \cdot \exp\left(j\frac{2\pi}{N}(n-1)\cdot\phi\right)\right| \\ &= N\cdot A\cdot\left|\frac{\operatorname{sinc}\left[\pi\left(\phi - N\Delta f\frac{2d}{c}\right)\right]}{\operatorname{sinc}\left[\frac{\pi}{N}\left(\phi - N\Delta f\frac{2d}{c}\right)\right]}\right| \end{aligned} \tag{14}$$

It is clear from Eq. 14 that the peak of range spectrum appears at $\Phi = 2dN\Delta f/c$, the estimated distance d is given by

$$d = \frac{c\phi}{2N\Delta f}, \tag{15}$$

where the maximum detectable range d_{max} is given by $c/2\Delta f$.

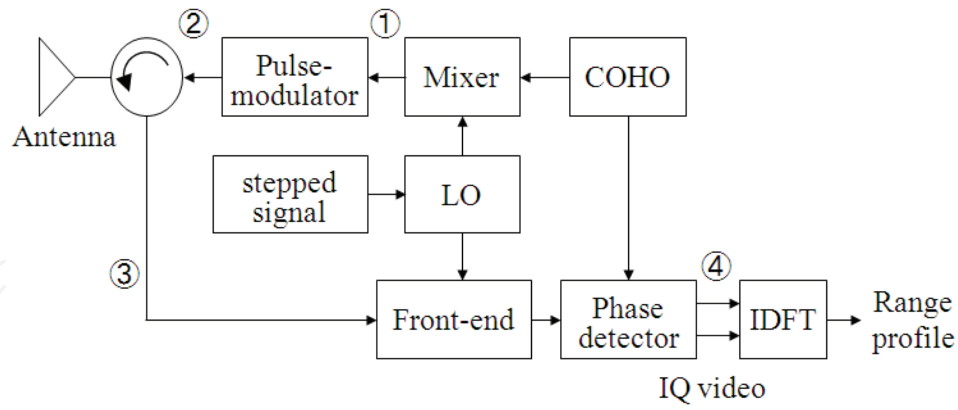

(a) Block diagram

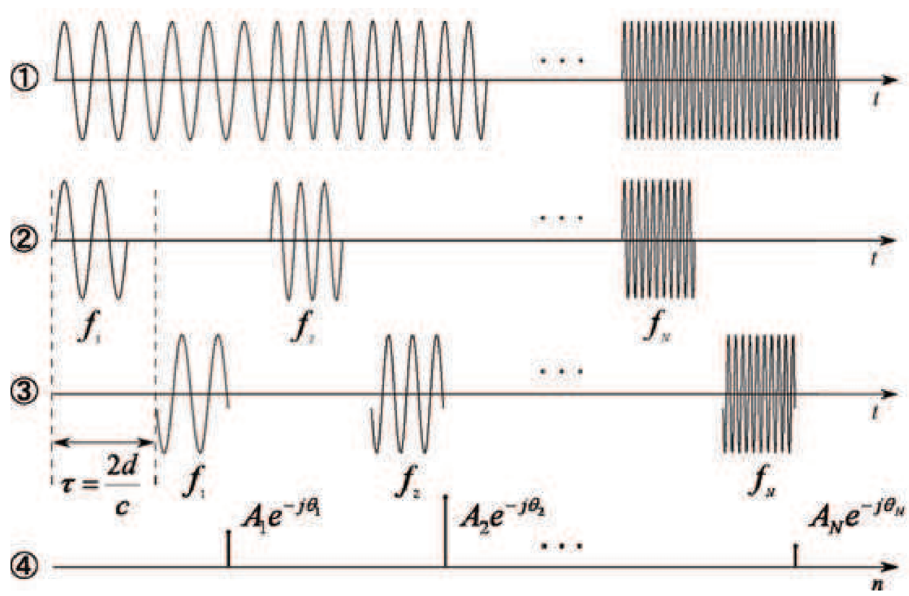

(b) Signal waveforms

Fig. 7. Block diagram and signals

3.2 Spectrum hole

The stepped-FM scheme also offers spectrum hole (non-activated within a portion of the radio spectrum) since it consists of independent pulses with different frequency. Thus it is expected to coexist with the existing systems (Nakamura et al., 2011).

Fig.8 shows the power spectrum for $\Delta f = 34.5$MHz and N=30 where the stepped-FM pulses with the spectrum-hole of 69MHz from 3.655 to 3.724GHz 6.6% (corresponding to two consecutive stepped pulses) are not transmitted. The holed band is seen to be by approximately 13dB suppressed relative to the signal spectrum. Consider the FCC regulation of -41.3dBm/MHz, the normalized spectrum of the holed band is less than -55dBm. Therefore it should not interfere with the existing systems unlike a UWB-IR. Fig. 9 shows the range spectrum for a point target at 2.2m where we assumed a spectrum-hole of 6.6% (69MHz band as 3.655~3.724GHz) and a zero-padding for the IDFT processing (1,024points). Remarkable degradation of range-resolution is not seen, although the range side-lobe is degraded.

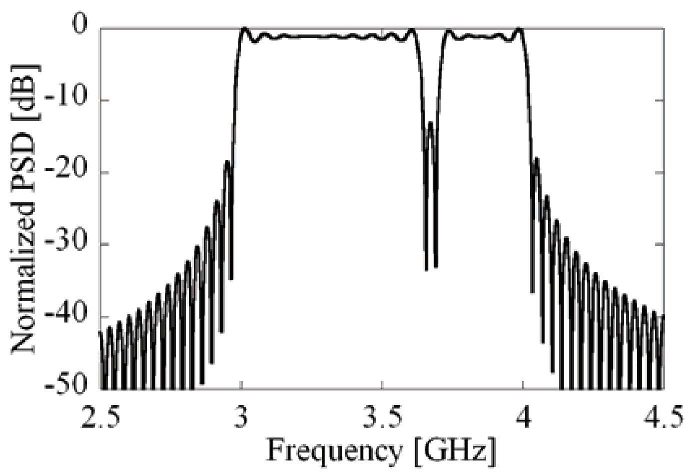

Fig. 8. Power spectrum of transmit signal with spectrum-hole of 6.6%

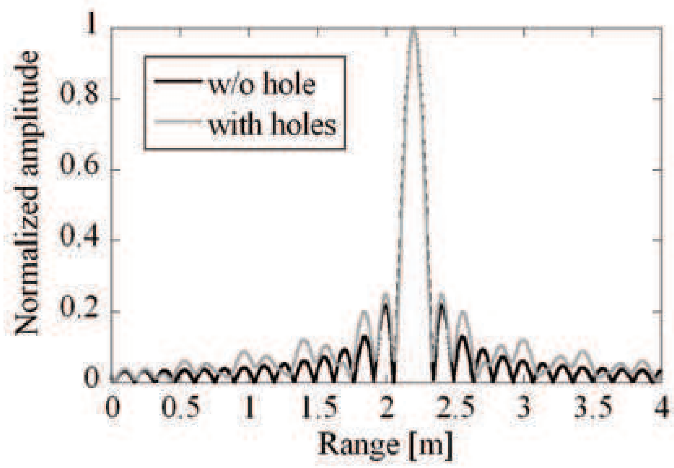

Fig. 9. Range spectra with and without hole. A point target is placed at 2.2m

3.3 Effect of spectrum-hole

The effect of spectrum-hole on the range spectrum is presented where the measurement specification is shown in Table 1. Two sphere targets with -9dBsm and -15dBsm are measured in an RF anechoic chamber (Skolnik, 2001) (Nakamura et al., 2011). The measurement was conducted in an RF absorber where theses targets on turn table were placed at 2.2m and 3m from the antenna. Fig.10 shows the range spectrum with spectrum-hole of 6.6%s, which is compared with that without hole. Please note that the other echoes at 0.8m and 1.6m are from the turn table. Fig.11 shows the range spectrum as a function of rotation angle where the distane from thsese targets to the antenna are almost equal at the rotation angle of 90 degree. These targets are found to be discriminated because of the range resolution of approximately 15cm. The measurements were conducted for $\Delta f = 34.5$MHz and N=30. Consider $\Delta f = 7.5$MHz and N=133, however, the maximum detectable range d_{max} is 20m and the range-resolution is approximately 15cm which is applicable to the short-range automotive radar.

From the measurement results, it can be concluded that the stepped-FM radar without high speed A/D devices can be coexistent with other narrowband wireless applications.

Frequency	3~4GHz
Stepped width Δf	34.5MHz
Number of step N	30
Stepped cycle	10msec
A/D	10kS/sec
IDFT point	1024

Table 1. Measurement specifications

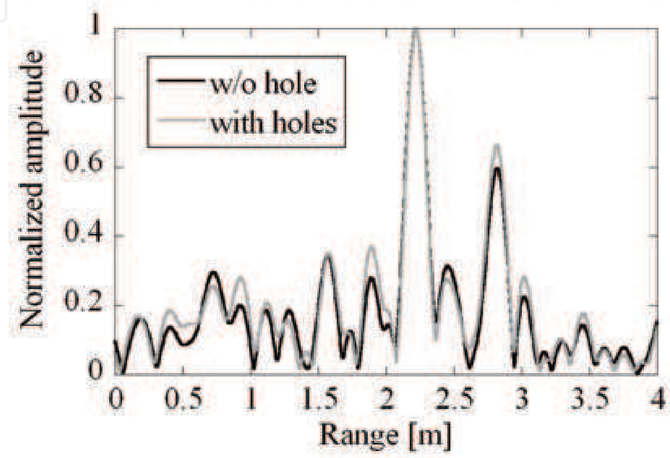

Fig. 10. Range spectra for two targets when the spectrum-holes is 6.6%

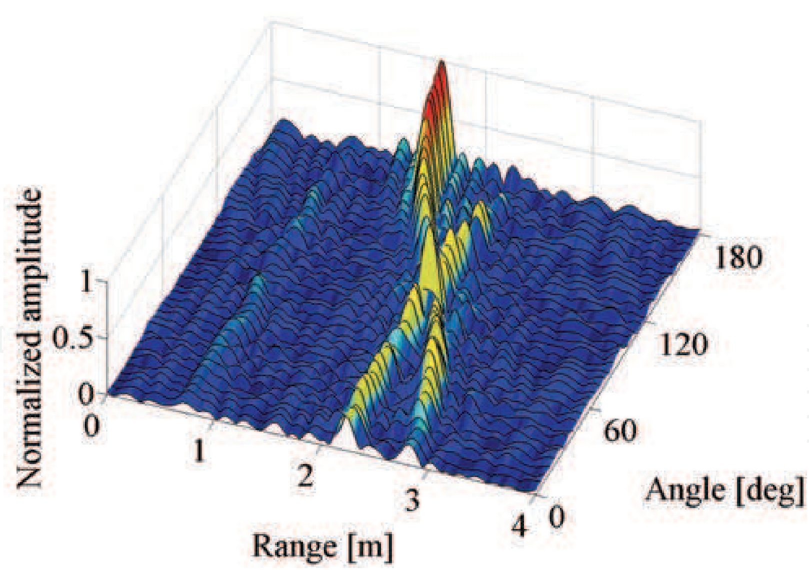

Fig. 11. Range spectrum as a function of for two sphere targets

4. Detection using trajectory estimation

Short-range automotive radar with high range-resolution should suffer from clutter because of its very broad lateral coverage. It is therefore an important issue to detect moving automobile in heavy clutter conditions. The clutter may be generally classified from automobile by the Doppler, but it will be difficult for a very short-pulse of UWB-IR radar. This is because a shorter pulse will have better range-resolution, but poorer Doppler resolution. Observing the range profile during several micro-seconds, however, each object echo's trajectory is estimated using Hough transformation and the Doppler is then calculated (Okamoto et al., 2011). When the speed of object is almost constant during the time, for example, the trajectory is regarded as linear on the time-range coordinate (Hough space). As a result, moving automobiles are separated from stationary clutter in the Hough space and detected/tracked with high range. The field measurement results at 24GHz are presented.

4.1 Time-range profile

Fig.12 shows an example of received range profile on a roadway for a bandwidth of 1GHz. The profile includes many echoes distinguishable with different delay. Detection, recognition and tracking of automobile in clutter are very important issues in automotive radar. Traditionally, the received range profile for each transmit pulse is compared against a given threshold and a detection decision is made. And once the decision is successfully done, the range profile is discarded and the next one is considered. This is called threshold detection. However it is not easy to detect some automobiles simutaneously in heavy clutter because the automobiles can't be distinguished from clutter in frequency domain. A time-range profile based detection is useful for the UWB-IR radar where moving automobiles are classified from clutter by observing the range profile. Fig.13 shows the range profiles as a function of transmit pulse number, which is called time-range profile. It is seen from Fig.13 that each echo's trajectory may be estimated and the Doppler is then calculated.

4.2 Hough transform

Hough transform (HT) has been widely applied for detecting motions in the fields of image processing and computer vision. Consider the time-range profile as shown in Fig.13, the time trajectory of each object echo can be estimated by the HT, which is a computationally efficient algorithm in order to detect the automobile on time-space data map. For example, the trajectory would be linear for a short duration of 0.1 second or less, thereby the Doppler can be calculated from the inclination of line.

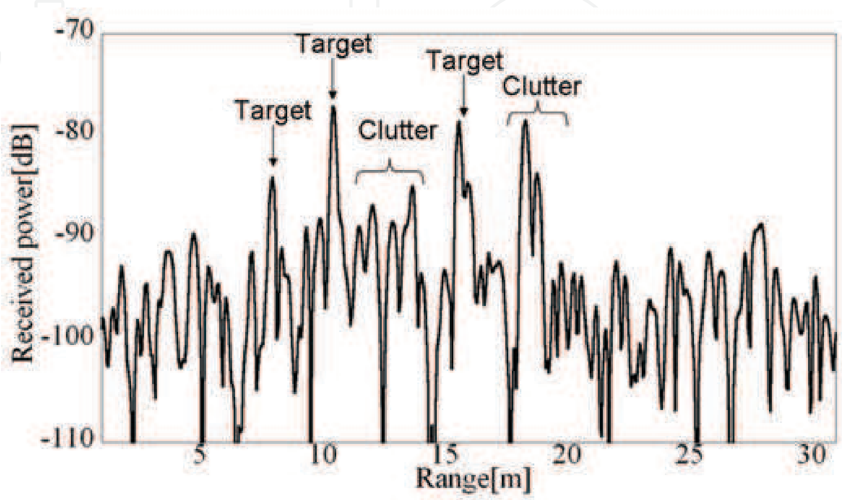

Fig. 12. Power range profile for a roadway

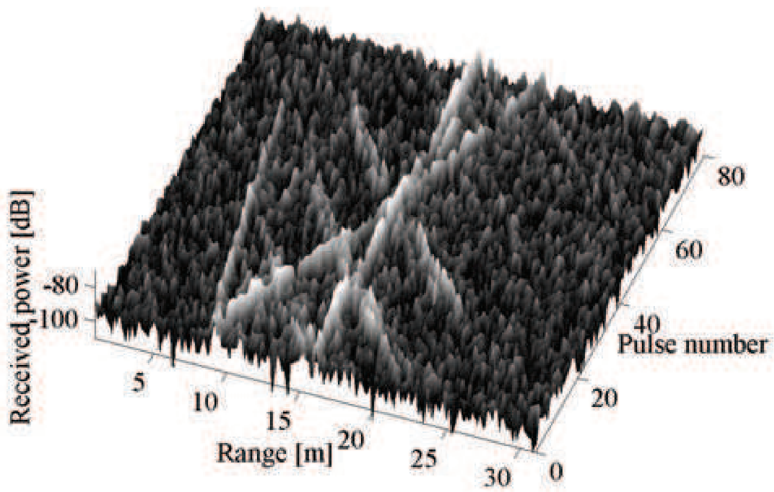

Fig. 13. Time-range profiles for 50 nanosecond pulses

4.3 Automobile classification

A. Measurement set-up and procedure

The measurements were conducted on a roadway as shown in Fig.14. The detail specification is shown in Table 2. The four automobiles were driven along the roadway and the received signals were processed on board. A pulse repetition interval (PRI) of 15ms is considered for the scenario of Fig.14. The antennas with a beam-width of 70° in horizontal direction were placed 60cm above the ground. Please note the anti-collision radar is designed for short-range/wide-angle object detection.

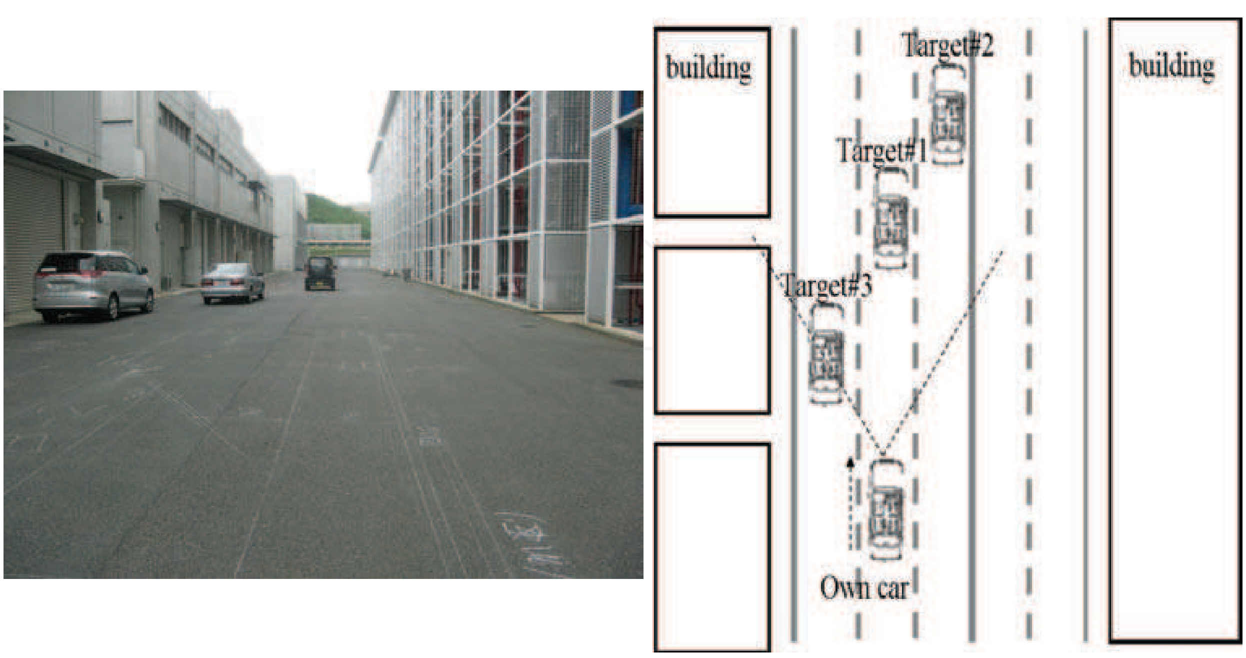

(a) Measurement scene (b) Measurement scenario

Fig. 14. Measurement scenario

Bandwidth	5GHz, 1GHz（centered at 24GHz）	
Antenna	Polarization	H-H. plane
	Type	Double-ridged Horn
	Gain	12.5dBi（24GHz）
	Height	60cm
Target	Sedan: #1	4.64m×1.72m×1.34m
	SUV: #2	4.42m×1.81m×1.69m
	Mini-van: #3	4.58m×1.69m×1.85m

Table 2. Measurement parameters

B. Measurement results

Fig.15 shows the flow of HT algorithm from time-range profile to trajectory line. The quasi-images (8bits time-range image) for BW=300MHz and 500MHz are shown in Fig.15(a) and (b) respectively. Many trajectories are plotted by the Hough space translation. The number of trajectory lines depends on the signal-to-clutter ratio (SCR) and the window size to observe the time-range profile. Some trajectory lines of a time-range profile would be connected to the lines of the following profile. Therefore the trajectory of object echo can be selected using the continuity between the consecutive time-range profiles, while the quasi trajectory should be discarded. Fig.16 (a) shows the estimated trajectory lines for a BW of 500MHz. It is seen that many lines are depicted because of significant clutter. Fig.17(b) shows the survived lines by the algorithm of Fig.15 where three time-range profiles for 20 pulses are used. It is seen that clutter can be estimated from the Doppler. Fig.18 also shows the estimated lines for a BW of 300MHz. The results of Figs. 17and 18 are found to agree with the scenarios. The measurements were also conducted for different scenarios of side-looking and back-looking radar and the trajectory estimation scheme is found to be useful in order to classify the automobile from heavy clutter.

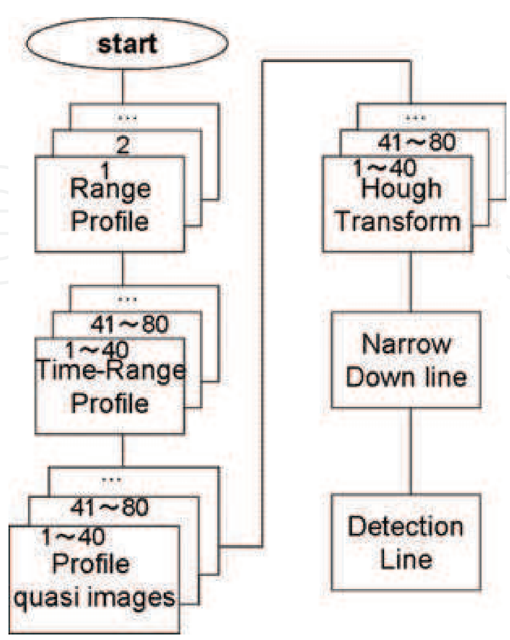

Fig. 15. Signal flow for HT algorithm

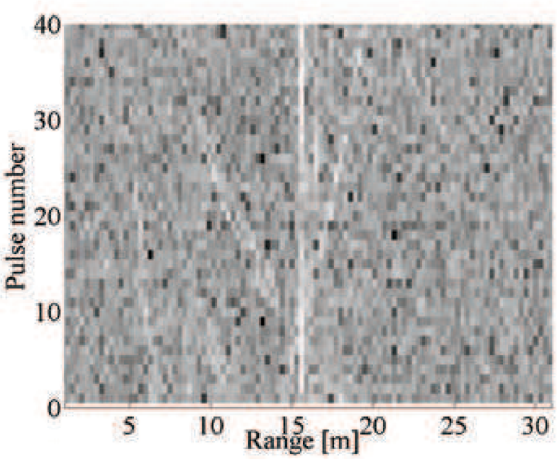

(a) BW=500MHz

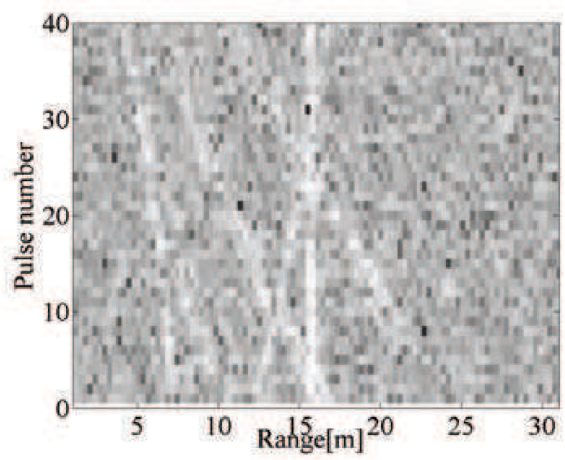

(b) BW=300MHz

Fig. 16. Quasi-images of time-range profile

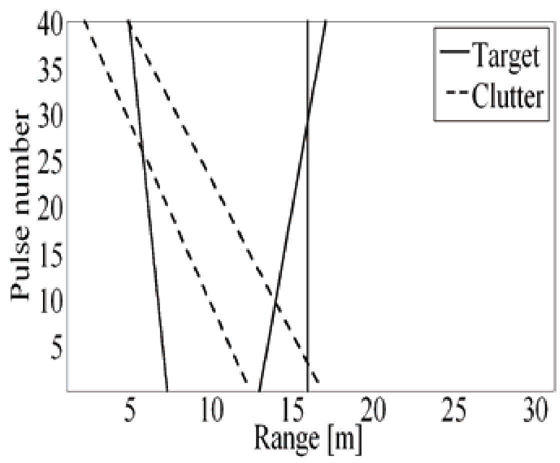

(a) Estimated trajectory lines by HT

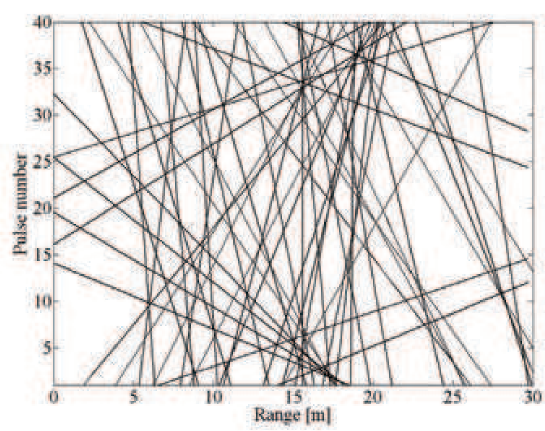

(b) Survived trajectory lines

Fig. 17. Estimated trajectory line (BW=500MHz)

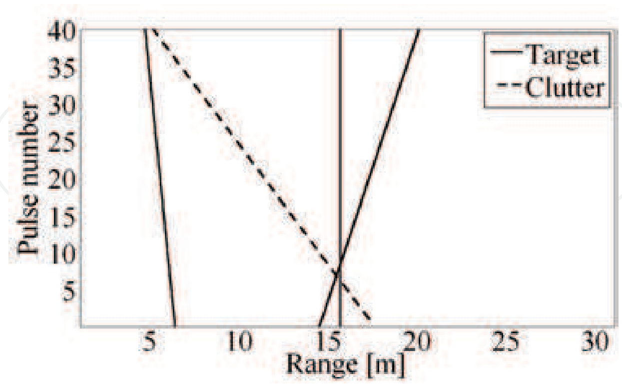

Fig. 18. Estimated trajectory line (BW = 300MHz)

5. Target discrimination

Automotive radar is required to detect automobile accurately, but not to detect clutters falsely, even in complicated traffic conditions. One-dimensional range profile of an automobile target has dependence on the shape because it has some remarkable scattered centers. Therefore the different types of automobile has different range profile feature which can be used as a unique template for automobile target discrimination/identification purpose in tracking mode. That is, the target is detected accurately by the correlation of received signal with template. The scheme also offers real-time operations unlike two-dimensional image processing (Overiez et al., 2003) (Sato et al., 2006). The measurement results are presented for various types of automobile (Matsunami et al., 2009) (Matsunami et al., 2010).

5.1 Target discrimaination and identification

Figs.19(a)-(c) show the measured range profile for various bandwidths where a sedan typed automobile was placed at approximately 10m. Please note that the profiles are expressed as a function of range-bin corresponding to the range-resolution (=1/BW). Echoes from various objects are found to be distinguished for wider bandwidth. It is seen that there exist some remarkable scattered centers. However the feature is not so clear because of scintillation and noise. Figs.20-22 show range profiles for various bandwidth where the non-coherent integration of 50 pulses was conducted in order to reduce the scintillation and noise. For the dedan, some strong echoes are seen from the side mirror and interior, and the SUV shows a unique feature.

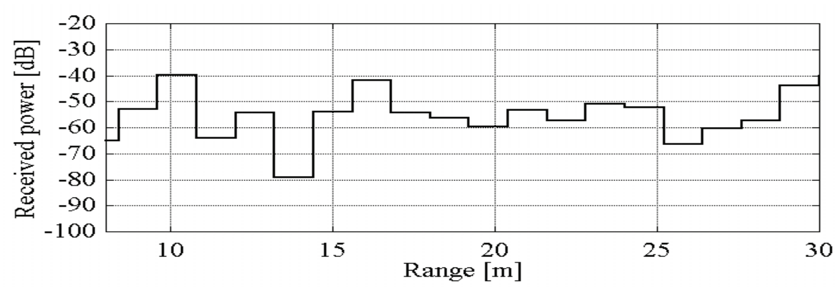

(a) BW=500MHz

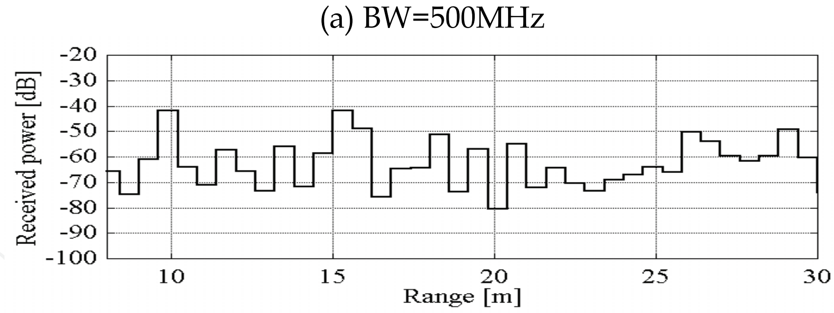

(b) BW=1GHz

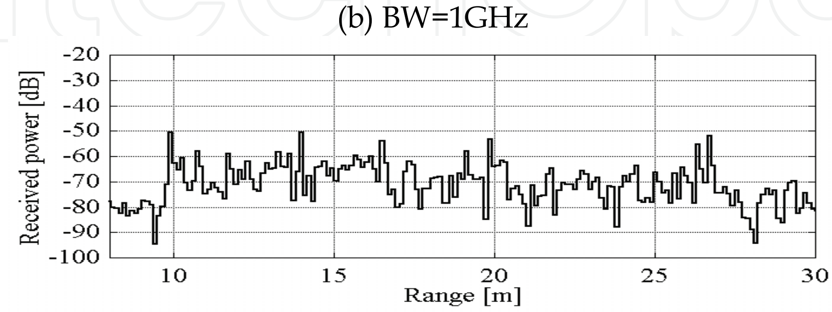

(c) BW=5GHz

Fig. 19. Power range profiles for various values of BW. A sedan was placed forward the radar antenna where the antenna to target separation was approximately 10m

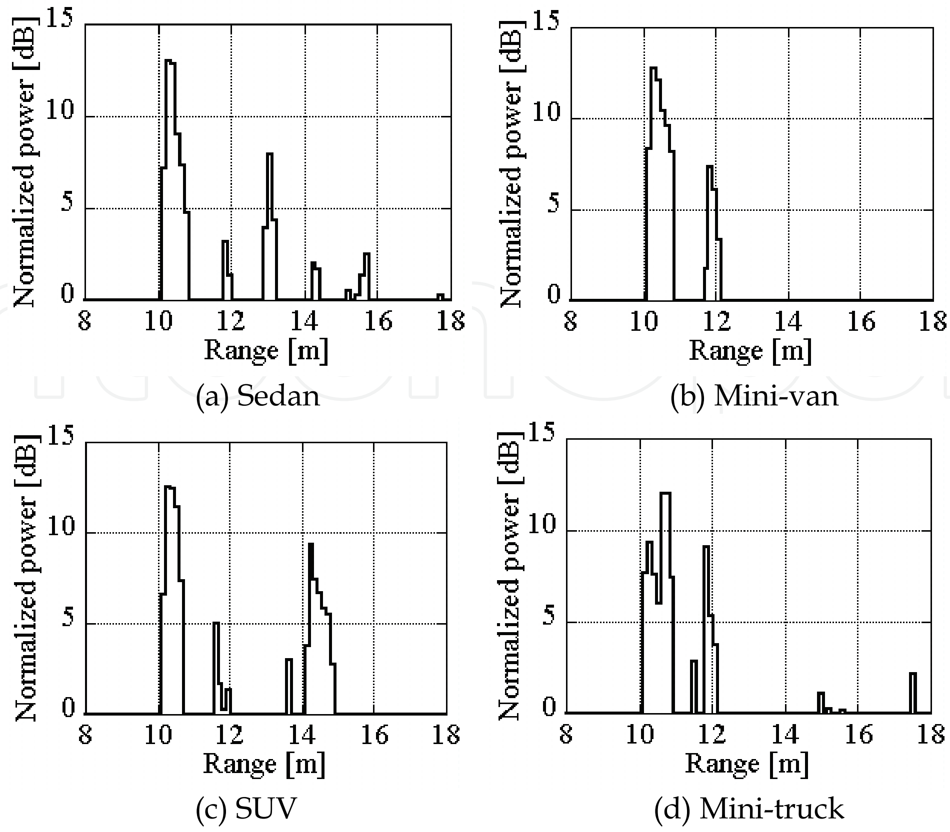

Fig. 20. Unique profiles of automobile (BW=5GHz)

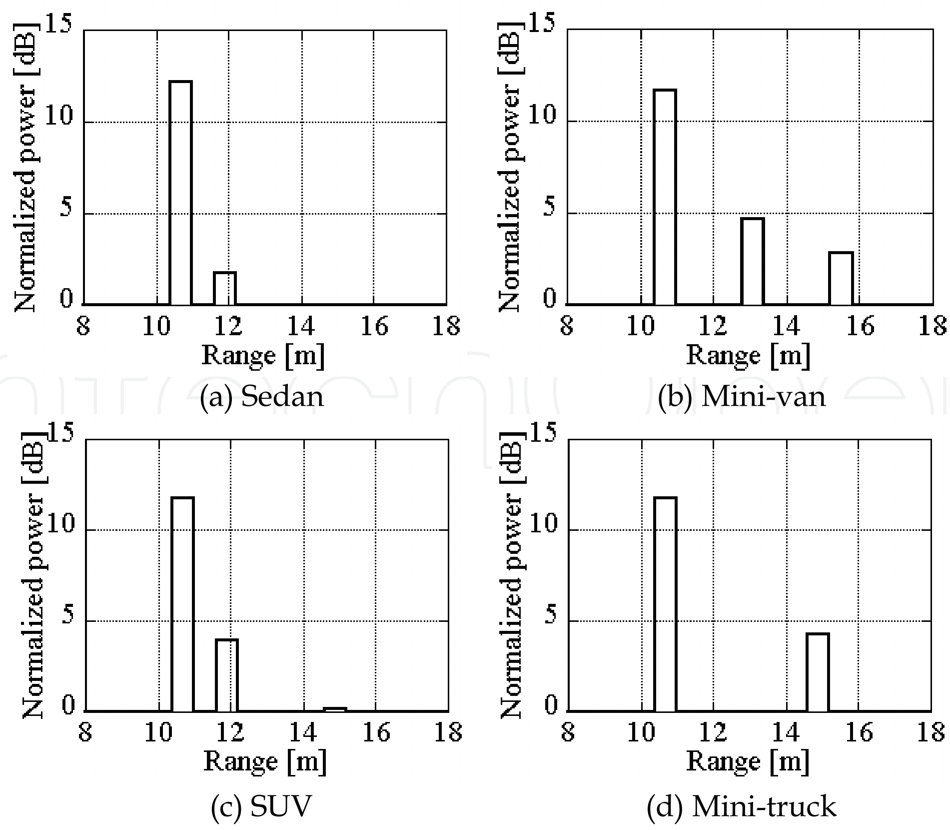

Fig. 21. Unique profiles of automobile (BW=1GHz)

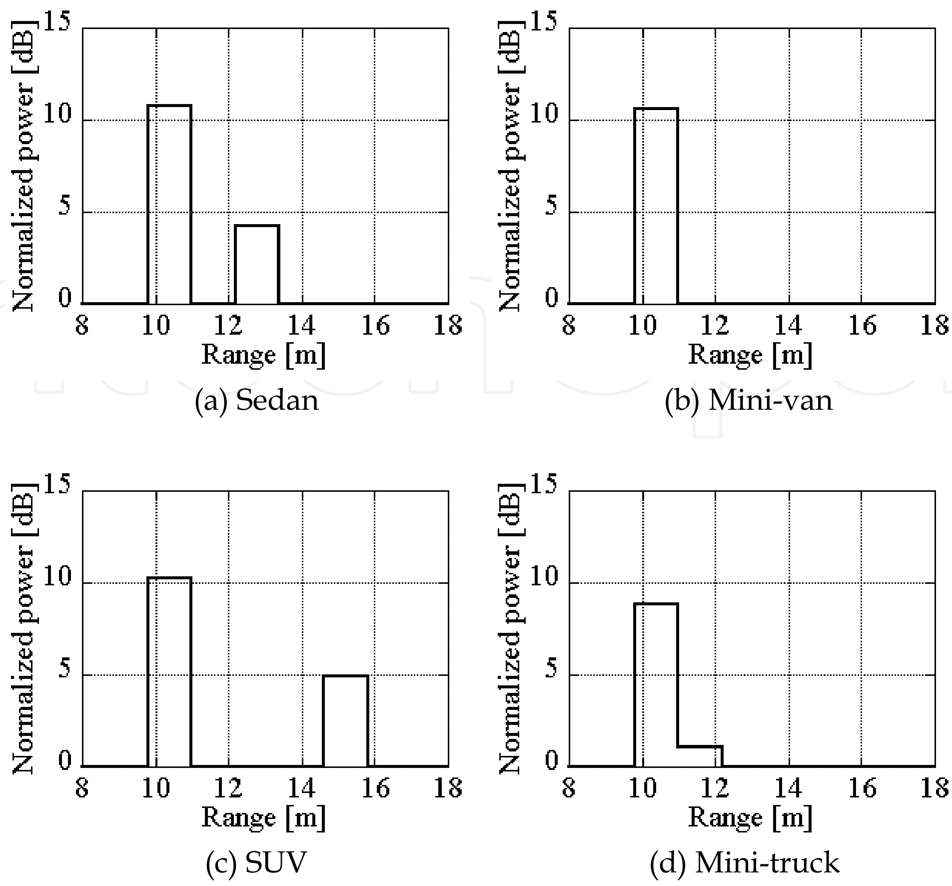

Fig. 22. Unique profiles of automobile (BW=500MHz)

5.2 Profile matching

Range profiles have been measured for four automobile #1~#4 (sedan, mini-van, SUV and mini-truck) which have been processed as the template. And the profile matching rate is calculated for various unknown automobiles. The matching rate is shown in Table.3-5. For BW=500MHz or more, it is higher than 96% when the automobile is the same as the template and each automobile can be detected. Assuming a correlation value of 0.6 for the discrimination, each profile can be identified in clutter since it has unique feature with god cross-correlation.

Template	Subject vehicle			
	Sedan	Mini-van	SUV	Mini-truck
Sedan	**99.1**	22.5	26.9	19.9
Mini-van	13.1	**96.9**	14.9	15.5
SUV	8.6	4.6	**98.6**	21.6
Mini-truck	16.8	20.8	15.3	**98.2**

Table 3. Matching rate [%] (BW=5GHz)

Template	Subject vehicle			
	Sedan	Mini-van	SUV	Mini-truck
Sedan	**99.4**	30.4	53.7	6.2
Mini-van	19.5	**96.0**	24.8	28.3
SUV	45.1	19.3	**99.3**	18.4
Mini-truck	14.7	24.8	31.7	**98.6**

Table 4. Matching rate [%]（BW=1GHz）

Template	Subject vehicle			
	Sedan	Mini-van	SUV	Mini-truck
Sedan	**99.9**	38.0	76.6	33.5
Mini-van	38.0	**98.9**	19.2	31.4
SUV	55.3	25.3	**98.2**	31.7
Mini-truck	31.2	20.0	33.0	**99.3**

Table 5. Matching rate [%]（BW=500MHz）

6. Conclusion

UWB-IR short-range radar a5 24/26GHz will be used for various applications such as pre-crash detection and blind spot surveillance. The short-range radar has a few significant problems to be overcome such as multiple targets detection and clutter suppression.
This chapter has presented how to detect multiple automobile targets in clutter. The presented results are as follows;

- UWB-IR radar requires high speed A/D devices to synchronize and detect the received nanosecond echo, thereby the system becomes very complicated and expensive. In section 3, the use of stepped-FM scheme which does not require high speed A/D has introduced for UWB-IR radar. In addition it offers spectrum hole to coexist with existing wireless systems.
- UWB-IR short-range radar is expected to provide a ***wide*** coverage in azimuth ***angle.*** Therefore, increased clutter makes it difficult to detect multiple automobile targets. Section 4 has introduced a multiple target detection scheme in heavy clutter using the trajectory of radar echoes.
- Section 5 has introduced a target identification scheme in order to improve the detection performance where a power delay profile matching is employed and the usefulness has been demonstrated by the measurement at 24GHz. The results have showed that automobile targets can be recognized and identified.

7. References

Skolnik, M. (2001). *Introduction to Radar systems, 3rd ed.*, McGraw-Hill, ISBN0-07-288138-0, New York

Taylor, J. D. (1995). Introduction to Ultra-wideband Radar Systems, CRC Press LLC, ISBN0-8493-4440-9, Wsshington, D.C..

Matsunami,I.; Nakahata, Y.; Ono, k. & Kajiwara,A. (2008). Empirical Study on Ultra-wideband Vehicle Radar, *Proc. of IEEE Vehicular Technology Conference,* ISBN 978-1-4244-1722-3, 8G-5, Calgary, Sept. 2008.

Nakamura,R.; Yokoyama,R. & Kajiwara,A. (2010), Short-Range Vehicular Radar Using Stepped-FM Based UWB-IR, *Proc. of IEEE Radio and Wireless Symposium*, ISBN 978-1-4244-4726-8, New Orleans, Jan. 2010.

Wehner, D. R. (1995). *High-Resolution Radar*, Artech House, ISBN978-0-89006-727-7, pp.197-255, 1995.

Nakamura,R. & Kajiwara,A.(2011), Empirical Study on Spectrum-Hole Characteristics of Stepped-FM UWB Microwave Sensor, to be appeared in *Proc. of* IEEE *Radio and Wireless Symposium*, Jan. 2011.

Okamoto,Y.; Matsunami,I. & Kajiwara,A.(2011), Moving vehicle discrimination using Hough, transformation, to be appeared in *Proc. of IEEE Radio and Wireless Symposium*, Jan. 2011.

Ovariez,J.P.; Vignaud,L.; Castelli,J.C.; Tria, M., & Benidir,M.(2003). Analysis of SAR image by multidimensional wavelet transform. *IEE Proc. Radar Sonar Navig.*, pp.234-241, Aug.2003.

Sato,T. & Sakamoto,T(2006). Reconstruction Algorithms for UWB Pulse Radar Systems, I*EICE Trans. Comm.*, ISBN1344-4697, vol.J88-B, pp.2311-2325, Dec.2006.

Matsunami,I. & Kajiwara,A.(2009). Power Delay Profile Matching for Vehicular Radar, *Proc. of IEEE Vehicular Technology Conference*, ISBN 978-1-4244-2514-3, 5E-1, Anchorage, Sept. 2009.

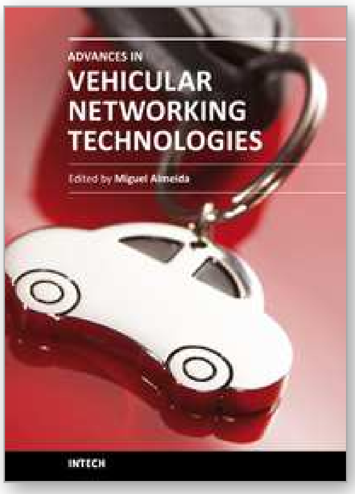

Advances in Vehicular Networking Technologies
Edited by Dr Miguel Almeida

ISBN 978-953-307-241-8
Hard cover, 432 pages
Publisher InTech
Published online 11, April, 2011
Published in print edition April, 2011

InTech Europe
University Campus STeP Ri
Slavka Krautzeka 83/A
51000 Rijeka, Croatia
Phone: +385 (51) 770 447
Fax: +385 (51) 686 166
www.intechopen.com

InTech China
Unit 405, Office Block, Hotel Equatorial Shanghai
No.65, Yan An Road (West), Shanghai, 200040, China
中国上海市延安西路65号上海国际贵都大饭店办公楼405单元
Phone: +86-21-62489820
Fax: +86-21-62489821